Carbohydrate Polymers 89 (2012) 46–53

Contents lists available at SciVerse ScienceDirect

Carbohydrate Polymers

journal homepage: www.elsevier.com/locate/carbpol

The target gene carrying validity to HePG2 cells with the brush-like glutathione modified chitosan compound

Congxin Li [a], Dezhong Zhou [a], Yuling Hu [a], Hao Zhou [b], Jiatong Chen [b], Zhengpu Zhang [a], Tianying Guo [a,*]

[a] Key Laboratory of Functional Polymer Materials (Nankai University), Ministry of Education, Institute of Polymer Chemistry, College of Chemistry, Weijin Road, No. 94, Tianjin 300071, China
[b] Department of Biochemistry and Molecular Biology, College of Life Science, Nankai University, Weijin Road, No. 94, Tianjin 300071, China

ARTICLE INFO

Article history:
Received 20 December 2011
Received in revised form 14 February 2012
Accepted 16 February 2012
Available online 5 March 2012

Keywords:
Modified chitosan
Glutathione
Nanocomplex
Non-viral gene vector
Targeted

ABSTRACT

The grafting modified chitosan with L-glutathione (GSH) end capped PEG brush-like poly [poly(ethylene glycol) methacrylate] (PMPEG), CS-PMPEG-GSH, as the pDNA condensed vector material could result in a much higher transfection efficiency and lower cytotoxity for NIH3T3 cells. In this work, we have further examined the morphology stabilities of CS-PMPEG-GSH/pDNA vectors at different medium pH values and in the presence of serum protein in detail. And then the targeted characters for HepG2 cells have been probed by tracing the cell uptake behavior and transfection efficiency.

1. Introduction

It is possible to predict that gene therapy will be the innovative therapy for the human being diseases in the future, especially for grievous diseases such as cancer, acquired immunodeficiency syndrome (AIDS) and hematophilia (Bhattacharya & Bajaj, 2009; Mintzer & Simanek, 2009; Salem, Searson, & Leong, 2003). Compared with viral vectors, non-viral vectors are safe, simple to prepare and modify, and have larger gene encapsulation capability, so they are more and more attractive in gene delivery systems (Bonamassa & Liu, 2010; Morille, Passirani, Vonarbourg, Clavreul, & Benoit, 2008; Rorke, Keeney, & Pandit, 2010).

Chitosan is a very important naturally occurring polysaccharide derived from the deacetylation of chitin, and has been used extensively in pharmaceutics due to its excellent biocompatibility and biodegradability. Chitosan is also one of the most successful and efficient non-viral vector materials because of its atoxicity, multiple functionalization and positive characteristics (Borchard, 2001; Hoffman & Stayton, 2007; Muzzarelli et al., 2012; Pack, Hoffman, Pun, & Stayton, 2005). However, pristine chitosan is still limited as a gene carrier because of its non-specific interactions, weak targeting and low transfection efficiency (Kievit et al., 2009; Muzzarelli, 2010; Ravi Kumar, Muzzarelli, Muzzarelli, Sashiwa, & Domb, 2004; Sun et al., 2008; Veiseh et al., 2005). In order to prevent non-specific protein adsorption, hydrophilic polymers such as poly (ethylene glycol) (PEG) were introduced. It is thought that PEG chains out of polyplexes are capable of reducing its interactions with blood and extracellular components (Ogris, Brunner, Schuller, Kircheis, & Wagner, 1999; Oupicky, Ogris, & Seymour, 2002). PEGylation not only reduces the plasma clearance by lung endothelia uptake and extends circulation time of CS-based polyplexes but also protect DNA degradation from plasma nucleases when used in systemic gene delivery (Gref et al., 2000; Kircheis et al., 1999). It is known that CS/pDNA complexes have positive charges and most cells have rich negative charges under physiological conditions, therefore, the endocytosis of CS/pDNA complexes is mainly conducted through the electrostatic interaction between the cell membrane and complexes. In this respect, all cell lines have the same chance of internalization complexes. As an ideal gene vector in clinical application, the most important prerequisite is to increase the specific uptake efficiency and to decrease the non-specific uptake efficiency. An efficient strategy for achieving this goal would be to add targeting ligands to polyplexes which would enhance their cell-specific gene delivery via receptor-mediated cellular uptake (Fernandez-Megia, Novoa-Carballal, Quinoa, & Riguera, 2007; Ogris et al., 2003). Many works have coupled cell targeting ligands, such as RGD peptides and folic acid onto cationic polymer vehicles in order to target integrin receptors on the cell surface (Cho et al., 2005; Kunath, Merdan, Hegener, Häberlein, & Kissel, 2003; Leamon & Low,

* Corresponding author. Tel.: +86 22 235 015 97; fax: +86 22 235 015 97.
E-mail address: tyguo@nankai.edu.cn (T. Guo).

0144-8617/$ – see front matter © 2012 Elsevier Ltd. All rights reserved.
doi:10.1016/j.carbpol.2012.02.035

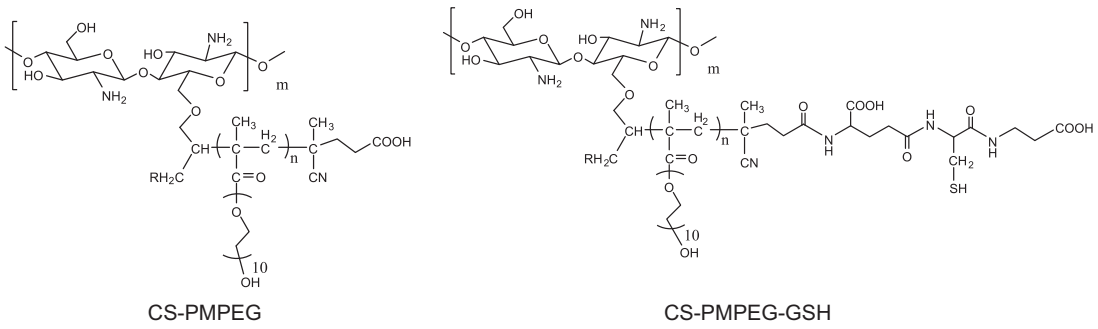

Scheme 1. Structure formulae of CS-PMPEG-GSH, CS-PMPEG.

2001; Tian et al., 2010, 2011; Zhang et al., 2010). These studies all indicate that conjugating a target ligand to gene carriers can effectively increase specific transfection efficiency to some kind of cells.

Glutathione in its reduced form (GSH), a small tripeptide formed by glutamic acid, cysteine and glycine, widely presenting in a variety of animal tissues, can role as specific peptide ligand to promote cell adhesion. Meanwhile, free thiol group is able to chelate divalent metal ions, which are essential to DNase for its activity (Krezel & Bal, 2003). In the previous work, we have designed a GSH modified chitosan compound, CS-PMPEG-GSH (the structure as shown in Scheme 1), using well-defined brush-like PMPEG polymers as spacer, and confirmed preliminarily that the gene vector based on this new material show superior performance both in cellular uptake and transfection efficiency for NIH3T3 cells compared to chitosan (Li et al., 2011). In this work, we further investigated the specific interactions of CS-PMPEG-GSH/pDNA gene vector to HeLa and HepG2 cells. At the same time the stability at the different physiological environments, cytotoxicity and in vitro transfection efficiency have been further probed for this vector system. And then the targeting assessments of the vector to HepG2 cells were performed on the transfection process, including monitoring of cellular uptake and transfection efficiencies among three cells lines, so as to probe into the prospect and direction of the material in clinical application.

2. Experimental

2.1. Materials and reagents

Chitosan was purchased from Gold-Shell Biochemical Co. Ltd. (*M*w = 50 kDa, degree of deacetylation (DD) =90%, Zhejiang, China).

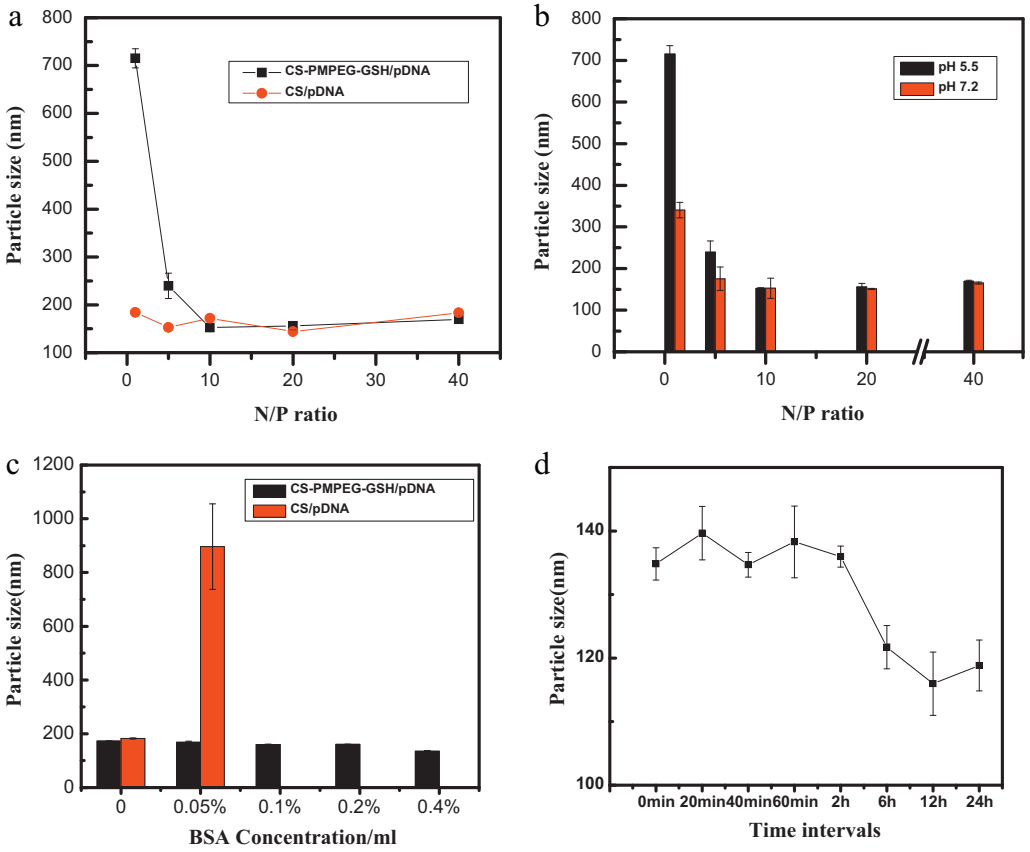

Fig. 1. (A) Effects of N/P ratios on the sizes of CS/pDNA and CS-PMPEG-GSH/pDNA complexes; (B) effect of pH on the size of CS-PMPEG-GSH/pDNA; (C) effect of BSA on the size of CS-PMPEG-GSH/pDNA complex; (D) effect of time on the size of CS-PMPEG-GSH/pDNA + 0.4%BSA. All experiments were done in triplicate and error bars represent mean ± S.D.

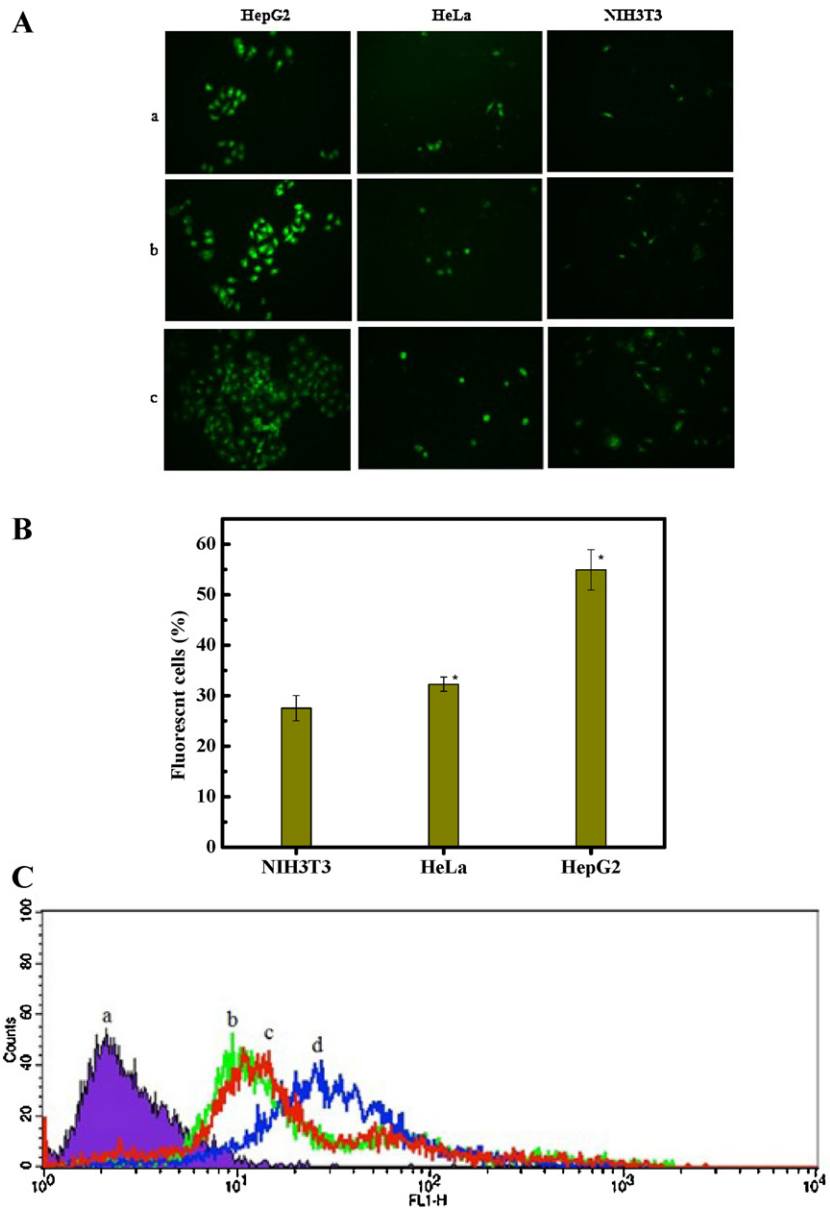

Fig. 2. Cell uptake of CS-PMPEG-GSH/pDNA complex in three cells. (A) Fluorescence images of three cells lines incubated with CS-PMPEG-GSH/pDNA nanoparticles for different time intervals (a) 30 min; (b) 2 h; (c) 4 h. (B) Cellular uptake rate of CS-PMPEG-GSH/pDNA in different cells lines following incubation for 4 h. Column and scatter referred to percentage of fluorescence-positive cells (%) and mean fluorescence intensity per cell, respectively. Significant difference from NIH3T3 cells: $p < 0.05$. Indicated values were mean ± S.D. of three experiments. (C) Fluorescence histograms of different cells (b, green, NIH3T3 cells) (c, red, HeLa cells) (d, blue, HepG2 cells) after incubation with FITC-CS-PMPEG-GSH/pDNA nanoparticles for 2 h, and the background of HepG2 cells (a, violet). (For interpretation of the references to color in this figure legend, the reader is referred to the web version of this article.)

CS-PMPEG-GSH and CS-PMPEG compounds were synthesized in our lab as previous report (Li et al., 2011), and the structure is shown in Scheme 1. Trypsin-EDTA, agarose, Dulbecco's modified Eagle medium (DMEM), fetal bovine serum (FBS) and 3-(4,5-dimethylthiazol-2-yl)-2,5-diphenyltetrazoliumerma bromide (MTT) were obtained from DingGuo Biotech. Co. Ltd. (Tianjin, China). Branched polyethylenimine (PEI, 25 kDa) were purchased from Sigma (St. Louis, MO). The plasmid pEGFP-N1 (4.7 kb; Clontech, Palo Alto, CA, USA) encoding enhanced green fluorescent protein (EGFP) is driven by immediate early promoter of CMV. The plasmid DNA (pDNA) was maintained and propagated in DH5α strain of *Escherichia coli*. The plasmids were purified by use of the Endfree plasmid kit (Tiangen, China), and purity and concentration of plasmids were confirmed by spectrophotometer (A260/A280).

2.2. Stability of CS-PMPEG-GSH/pDNA complexes

The stability of CS-PMPEG-GSH/pDNA complexes was detected by particle size analysis. The particle size of CS-PMPEG-GSH/pDNA complexes was assessed by laser particle size analyzer (Nano-ZS90, Malvern). The average particle size was expressed as the volume mean diameter *n*vd (nm). To study the serum stability of the complex nanoparticles, CS-PMPEG-GSH/pDNA complexes with N/P ratio 10 were first determined. The N/P ratios of chitosan or its derivative/pDNA complexes were expressed as the molar ratios of amine group of chitosan or its derivative to phosphate group of pDNA. Then, different concentrations of BSA (bovine serum albumin) were added into nanoparticle solution, and the particle size was measured at intervals.

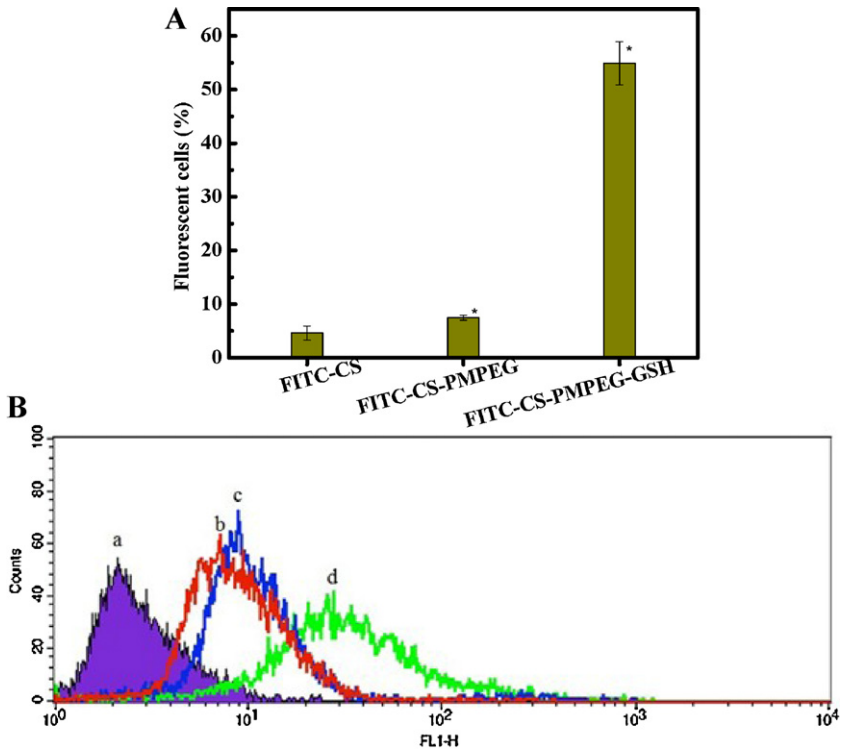

Fig. 3. (A) Cell uptake of CS/pDNA, CS-PMPEG/pDNA and CS-PMPEG-GSH/pDNA complexes in HepG2 cells following incubation for 4 h. Column and scatter referred to percentage of fluorescence-positive cells (%) and mean fluorescence intensity per cell, respectively. Significant difference from FITC-CS: $p < 0.05$. Indicated values were mean ± S.D. of three experiments. (B) Fluorescence histograms of HepG2 cells after incubation with CS/pDNA (b) and CS-PMPEG/pDNA nanoparticles (c) CS-PMPEG-GSH/pDNA nanoparticles (d) for 4 h, and the background of HepG2 cells (a).

2.3. Cell culture

The human cervical cancer cell line (HeLa), human hepatoma cell line (HepG2) and mouse embryonic fibroblast cell line (NIH3T3) were purchased from ATCC (Teddington, UK) and maintained in DMEM containing 10% FBS, 100 U/mL penicillin and 100 μg/mL streptomycin without using any antibiotics at a 37 °C and 5% CO_2 atmosphere.

2.4. Cellular uptake of CS-PMPEG-GSH/pDNA complexes

NIH3T3 cells, HeLa cells and HepG2 cells were maintained in DMEM supplemented with 10% fetal bovine serum (FBS), streptomycin (100 U/mL culture medium), penicillin (100 U/mL culture medium) at 37 °C, 5% CO_2 and 95% relative humidity. The cells were trypsin digested, collected, counted, and then seeded into 24-well plates containing coverslips at a density of 5×10^4 cells/well. After 24 h incubation, the cell monolayer was washed with DMEM, and FITC-CS-PMPEG-GSH/pDNA complexes with N/P 10 were added. At the time points indicated, the cells were viewed under an inverted fluorescence microscope and the images recorded with a CCD camera (Nikon ECLIPSE TE2000-U, Japan). After 4 h incubation, the cells were washed three times with PBS to remove the free FITC-labeled nanoparticles and harvested by trypsinization. The intracellular fluorescence intensity was measured with a flow cytofluorometer (BD FACS Calibur, USA). Approximately 1.0×10^4 cells were counted to determine the trend of the FITC-labeled nanoparticles taken up by the three cells.

2.5. Transfection experiment

Prior to transfection, HepG2 cells were seeded in 24-well plates at a density of 1×10^5 cells per well in 1 mL DMEM and incubated for 24 h, yielding a cell density of about 80% confluence. Then, the media were replaced with fresh growth media (pH 7.2) containing CS-PMPEG-GSH/pDNA complexes at different N/P ratios. After 24 h incubation, medium was changed with complete medium and cells were incubated for an additional 48 h. Cells treated with CS/pDNA and CS-PMPEG/pDNA in fresh growth media (pH 7.2) for 48 h were studied as control. Untransfected cells and cells transfected with naked pDNA (2.5 μg/well) were used as negative control. HeLa Cells and NIH3T3 cells transfected with CS-PMPEG-GSH/pDNA (N/P ratio 10) were used as contrast. GFP-positive cells were viewed under an inverted fluorescence microscope and the images recorded with a CCD camera (Nikon ECLIPSE TE2000-U, Japan). To quantitatively study the transfection efficiency, HepG2 cells were collected and approximately 1.0×10^4 cells were counted and measured with a flow cytofluorometer (BD FACS Calibur, USA).

2.6. MTT assay

HepG2 cells were seeded in 96-well plates at an initial density of 8000 cells/well in 100 μL of DMEM complete medium. The experimental procedures and characterization methods were same as the previous report (Li et al., 2011). Three replicates were counted for each sample. The mean value was used as the final result.

2.7. Statistical analysis

Data are presented as mean values ± standard deviation (S.D.). Statistical tests were performed with the Student's t test. All statistical tests were two-tailed tests and the differences between variants were considered to be statistically significant if $p < 0.05$.

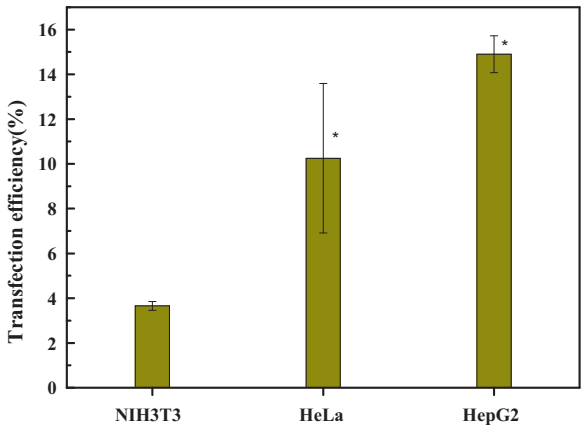

Fig. 4. Transfection efficiency of CS-PMPEG-GSH/pDNA complexes at N/P ratio 10 in three cells lines. Significant difference from NIH3T3 cells: $p < 0.05$. Each data point represents the mean ± S.D. of three replicates.

3. Results and discussion

3.1. Stability of CS-PMPEG-GSH/pDNA complexes

The hydrated diameters of the nanoparticles in aqueous solution are really very important because nanoparticles must be suitable for endocytosis of somatic cells. The mean diameter of CS/pDNA and CS-PMPEG-GSH/pDNA complexes as a function of N/P ratio was shown in Fig. 1A. At N/P ratio 1, CS-PMPEG-GSH/pDNA complexes would form large particles because of the inadequate positive charge for condensation of DNA. When the N/P ratio increases to 5, the particle sizes of CS-PMPEG-GSH/pDNA complexes decrease rapidly. At N/P ratio 10, CS-PMPEG-GSH showed best ability in DNA condensation, the mean diameter was about 150 nm. With increasing N/P ratio, the CS-PMPEG-GSH/pDNA complexes were stable and the mean diameter of particles was slightly larger than 150 nm. CS/pDNA complexes did not show obvious variation with the changes of N/P ratio. CS/pDNA complexes had the smallest particles at N/P ratio 5, the mean diameter was 152.8 nm. The polydispersity index of CS-PMPEG-GSH/pDNA complexes was 0.16 much lower than 0.21 of CS/pDNA complexes at N/P ratio 10.

The pDNA condensed nanoparticle vector must undergo the different intracellular and extracellular physiological environments during the gene delivery process, in which there are pH variations. Thus, the stability of nanoparticles in aqueous solutions (with different pH values) is very important for transfection process. As shown in Fig. 1B, the mean diameter of CS-PMPEG-GSH/pDNA complexes was significantly smaller in pH 7.2 than that in pH 5.5 both at low N/P ratio 1 and 5. This phenomenon indicates that the particle structure for CS-PMPEG-GSH/pDNA complexes at low N/P ratio is loosening since the lower density of CS-PMPEG-GSH on the complex particle surface. The uninvolved $-NH_2$ of the copolymer after pDNA condensing would be further protonated at pH 5.5, which will increase the repelling force between the polymer chains, and thus the particle size increases. On the contrary, for the complex at the higher N/P ratio, the formed pDNA condensed complex is compact in structure, and the strong hydrophilic PEG brushes would shield the complex off the effects of pH variation. The result demonstrated that the CS-PMPEG-GSH/pDNA complexes are stable at different physical environments, when N/P ratio is over 10, which is beneficial to the transfection process.

At the same time, the non-specific protein adsorption has a significant impact on the transport process of nanoparticles in vivo, such as, leading to "violent release" or incomplete release of the drug or reducing circulation time of nanoparticles (Cao & Shoichet, 1999; Landry, Bazile, Spenlehauer, Veillard, & Kreuter, 1996). In this

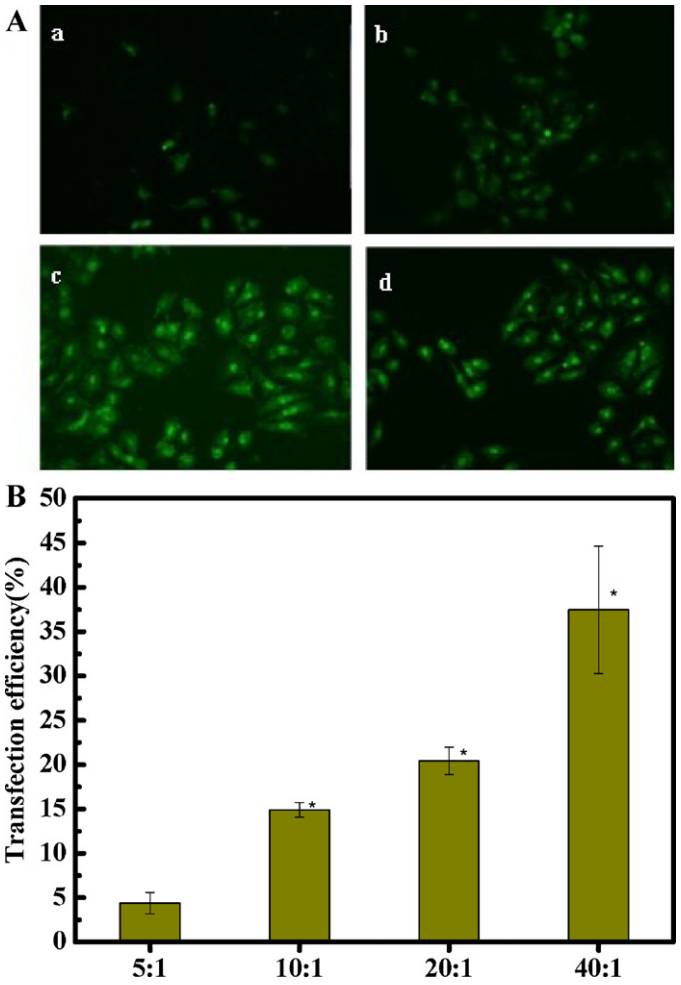

Fig. 5. In vitro transfection efficiency of CS-PMPEG-GSH/pDNA complex against HepG2 cells. Images of HepG2 cells with CS-PMPEG-GSH/pDNA complexes observed under fluorescent microscope (10× magnification) green field. CS-PMPEG-GSH/pDNA complexes were prepared at different N/P ratios: (a) 5; (b) 10; (c) 20; and (d) 40 (A); the effect of N/P ratio on the transfection efficiency of CS-PMPEG-GSH/pDNA complexes, each data point represents the mean ± S.D. of three replicates (B). (For interpretation of the references to color in this figure legend, the reader is referred to the web version of this article.)

work, BSA was chosen as an sample of non-specific proteins. The effect of different concentrations of BSA on the size of CS-PMPEG-GSH/pDNA (N/P 10) was probed. As shown in Fig. 1C, the addition of BSA almost has no effect on the particle size of CS-PMPEG-GSH/pDNA complex, but the sizes of chitosan/pDNA nanoparticles increased rapidly, when only 0.05% BSA was added into. When BSA concentration was increased to 0.1%, a large number of chitosan/pDNA nanoparticles precipitated. The result indicates that CS-PMPEG-GSH/pDNA complexes could effectively prevent the protein adsorption.

In the next step, the stability of CS-PMPEG-GSH/pDNA nanoparticles in 0.4% BSA/mL at different time intervals was examined. It is found in Fig. 1D that all particles are below 140 nm and the particle size decreases with time an hour later. These results demonstrate further that the CS-PMPEG-GSH/pDNA particles are stable without adsorbing non-specific protein, which is most possibly derived from the action of the brush-like PMPEG located on the outside of the particles and formed a hydrophilic layer in aqueous solution. The study on the stability of CS-PMPEG-GSH/pDNA complexes shows that CS-PMPEG-GSH has a great promising as an ideal gene vector in clinical application.

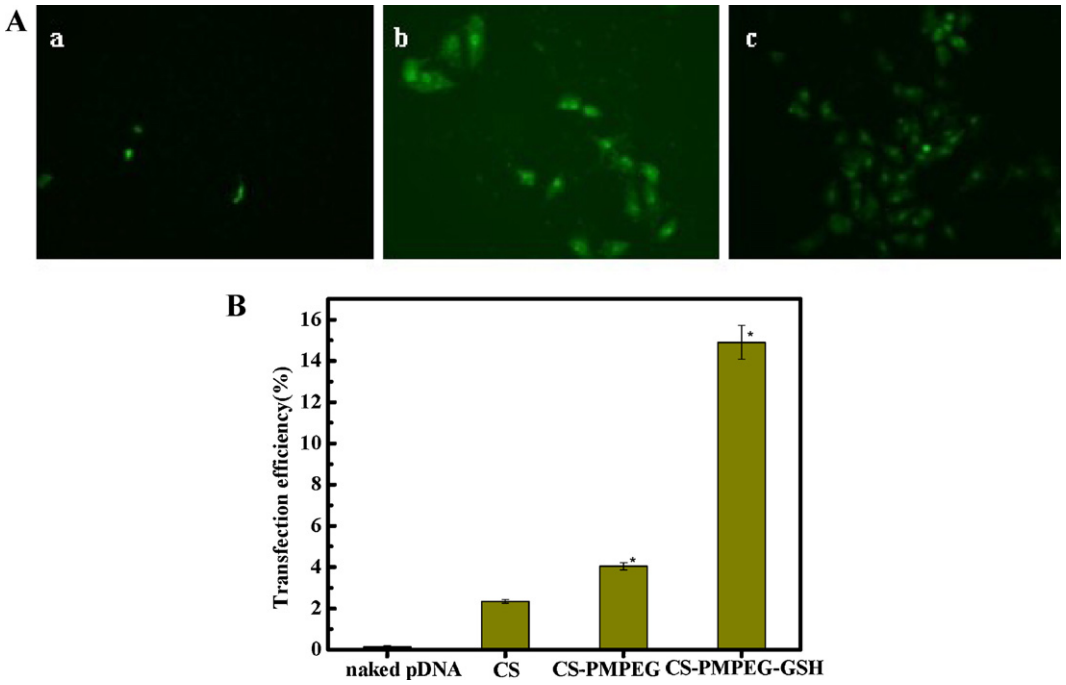

Fig. 6. EGFP expression in HepG2 after 48 h with an N/P ratio of 10. Images of HepG2 cells transfected with naked CS/pDNA (a), CS-PMPEG/pDNA (b) and CS-PMPEG-GSH/pDNA (c) complexes observed under fluorescent microscope (10× magnification) (A); transfection efficiency of CS-PMPEG-GSH compared with that of CS and CS-PMPEG at N/P ratio 10 and naked DNA. Significant difference from CS: $p < 0.05$. Each data point represents the mean ± S.D. of three replicates (B).

3.2. Cellular uptake of CS-PMPEG-GSH/pDNA complexes

Though the previous work (Li et al., 2011) has preliminarily proved that the cellular uptake rate of CS-PMPEG-GSH/pDNA in NIH3T3 cells was elevated by 2.0 folds compared to chitosan/pDNA complex just after 4 h incubation at the same N/P ratio 10, we still need to know its extensive representations for different cell lines. To study the cellular uptake rate of CS-PMPEG-GSH/pDNA complexes in three cell lines, the cells were incubated with FITC-CS-PMPEG-GSH/pDNA complexes for different intervals (from 30 min to 4 h). The fluorescence intensity of FITC-CS-PMPEG-GSH/pDNA complexes in HepG2 cells is higher than that in HeLa cells and NIH3T3 cells in every time point (Fig. 2A–C), which indicates that CS-PMPEG-GSH/pDNA complexes are apt to be uptaken by HepG2 cells than HeLa cells and NIH3T3 cells. To further study the cellular uptake rate of CS-PMPEG-GSH/pDNA complexes in these three cell lines, the cells after incubation with FITC-CS-PMPEG-GSH/pDNA complexes for 4 h were subjected to flow cytometry. The mean fluorescence intensity in HepG2 cells was the highest in the three cell lines which was even two times higher than that in NIH3T3 cells. About 56% of HepG2 cells showed uptake of the FITC-CS-PMPEG-GSH/pDNA nanoparticles. In comparison, only 32% of HeLa cells and 26% of NIH3T3 cells took up the FITC-CS-PMPEG-GSH/pDNA nanoparticles. These results indicate that the uptake rate of CS-PMPEG-GSH/pDNA complexes in HepG2 cells could be faster than in HeLa cells and NIH3T3 cells. We consider that the increased cellular uptake rate of CS-PMPEG-GSH/pDNA complexes in HepG2 compared to other two cell lines might be due to the stronger interaction between CS-PMPEG-GSH/pDNA complexes and cell membranes of HepG2 cells. The cellular uptake of FITC-CS-PMPEG-GSH/pDNA complexes was significantly higher than that of FITC-CS-PMPEG/pDNA and FITC-CS/pDNA complexes in HepG2 cells. The mean cellular uptake rate of HepG2 cells for the FITC-CS-PMPEG-GSH/pDNA nanoparticles and the FITC-CS-PMPEG/pDNA nanoparticles were 56% and 7%, respectively, indicating approximately a 7.0-fold improvement in cell uptake of the FITC-CS-PMPEG-GSH/pDNA nanoparticles. Therefore, we speculate that GSH plays a major role in the uptake of these nanoparticles, and the GSH modified nanoparticles have a higher affinity to the HepG2 cells. The higher cellular uptake of FITC-CS-PMPEG-GSH/pDNA complexes could result from the interactions sourced the sulfhydryl groups in GSH, which are capable of forming disulfide with the sulfhydryl-rich mucin glycoproteins on the cell membranes, thus leading to an increased cellular uptake rate (Lee et al., 2007; Loretz, Thaler, & Schnurch, 2007; Martien, Loretz, Thaler, Majzoob, & Schnürch, 2007; Schmitz et al., 2007; Zhao et al., 2010). The results show that the system has the potential to become a gene vector that could increase specifically the uptake efficiency to HepG2 cells (Fig. 3).

3.3. Transfection efficiency in vitro

The transfection efficiency for different cell lines of CS-PMPEG-GSH/pDNA complexes was first investigated at N/P ratio 10 (as shown in Fig. 4). The result shows that the highest transfection efficiency occurs in HepG2 cells which are agreement better with the result of cellular uptake rate. This suggests that the higher efficiency of endocytosis would result in the better transfection efficiency.

Next, for HepG2 cells, the influence of N/P ratio on the transfection efficiency for CS-PMPEG-GSH/pDNA complexes was investigated at four N/P ratios (N/P ratio 5, 10, 20 and 40). In Fig. 5 both the qualitative and quantitative results show an excellent transfection efficiency which increases with the increase of the N/P ratio.

To know further whether the modification of chitosan with GSH could increase its transfection efficiency in HepG2 cells, we compared the transfection efficiency of CS-PMPEG-GSH/pDNA complexes with that of chitosan/pDNA and CS-PMPEG/pDNA complexes. The results in Fig. 6 showed that the transfection efficiency of CS-PMPEG-GSH/pDNA complexes was significantly higher than chitosan/pDNA complexes. The increased transfection efficiency should be attributed to the increased cellular uptake of pDNA into the cells by the introduction of sulfhydryl group in GSH because the cell membrane is the first obstacle in cellular gene delivery, and

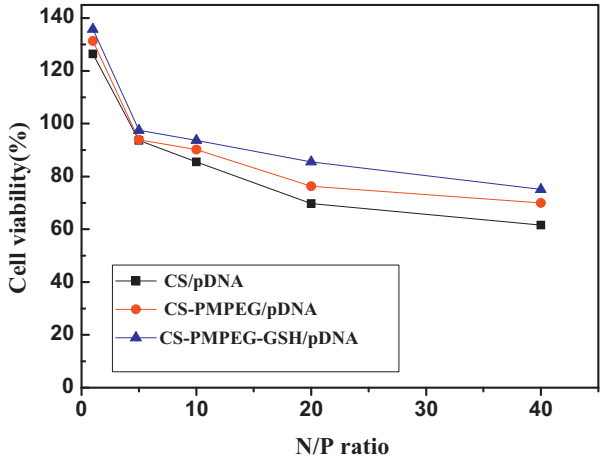

Fig. 7. Cytotoxicity of CS/pDNA, CS-PMPEG/pDNA and CS-PMPEG-GSH/pDNA at different N/P ratios against HepG2 cells after 24 h. Each data point represents the mean of three replicates.

the increasing pDNA internalization would increase the opportunity for nuclear delivery of pDNA. This result further suggests that the conjugated glutathione as a ligand to gene carriers plays a key role in the dramatic increase of transfection efficiency for HepG2 cells, which indicates that the system will be a promising approach for specific tumor gene therapy.

3.4. Cytotoxicity assay

The cytotoxicity of the CS-PMPEG-GSH/pDNA complexes was evaluated against HepG2 cell line by MTT assay. In Fig. 7, it is found that CS-PMPEG-GSH/pDNA complexes showed less cytotoxicity than CS-PMPEG/pDNA complexes and chitosan/pDNA complexes at the same N/P ratio. Even upon exposure of CS-PMPEG-GSH/pDNA complexes at N/P 40, about 85% cell viability is observed in HepG2 cells. These results demonstrate that CS-PMPEG-GSH is a very promising material for safe gene delivery in HepG2 cells.

4. Conclusions

The newly synthesized GSH and brushed PEG modified chitosan, CS-PMPEG-GSH compound as a novel gene delivery vector shows very high transfection efficiency for all three cell lines NIH3T3, Hela and HepG2. The brush-liked PMPEG and GSH groups modified chitosan could prevent self aggregation of complexes in the present of serum and increase binding ability with the cell membrane. In addition, with the lower toxicity, better pH and serum stabilities and higher uptake rate, the CS-PMPEG-GSH compound compared to pristine chitosan, shows much greater potential as an efficient and safe nonviral gene vector. And the higher uptake rate and transfaction efficiency of the compound to HepG2 cells indicate that this material has the potential to be a specific vector for liver cancer.

Acknowledgments

The authors were grateful to National Natural Science Foundation of China (Proj. No. 20874052) and State Key Lab for Modification of Chemical Fibers and Polymer Materials, Donghua University, China (Proj. No. LK 0808) for financial support.

References

Bhattacharya, S., & Bajaj, A. (2009). Advances in gene delivery through molecular design of cationic lipids. *Chemical Communications*, *31*, 4632–4656.

Bonamassa, B., & Liu, D. X. (2010). Nonviral gene transfer as a tool for studying transcription regulation of xenobiotic metabolizing enzymes. *Advanced Drug Delivery Reviews*, *62*, 1250–1256.

Borchard, G. (2001). Chitosans for gene delivery. *Advanced Drug Delivery Reviews*, *52*, 145–150.

Cao, X. D., & Shoichet, M. S. (1999). Delivering neuroactive molecules from biodegradable microspheres for application in central nervous system disorders. *Biomaterials*, *20*, 329–339.

Cho, K. C., Jeong, J. H., Chung, H. J., Joe, C. O., Kim, S. W., & Park, T. G. (2005). Folate receptor-mediated intracellular delivery of recombinant caspase-3 for inducing apoptosis. *Journal of Controlled Release*, *108*, 121–131.

Fernandez-Megia, E., Novoa-Carballal, R., Quinoa, E., & Riguera, R. (2007). Conjugation of bioactive ligands to PEG-grafted chitosan at the distal end of PEG. *Biomacromolecules*, *8*, 833–842.

Gref, R., Lück, M., Quellec, P., Marchand, M., Dellacherie, E., Harnisch, S., et al. (2000). 'Stealth' corona-core nanoparticles surface modified by polyethylene glycol (PEG): Influences of the corona (PEG chain length and surface density) and of the core composition on phagocytic uptake and plasma protein adsorption. *Colloids and Surfaces B: Biointerfaces*, *18*, 301–313.

Hoffman, A. S., & Stayton, P. S. (2007). Conjugates of stimuli-responsive polymers and proteins. *Progress in Polymer Science*, *32*, 726–753.

Kievit, F. M., Veiseh, O., Bhattarai, N., Chen, F., Gunn, J. W., Lee, D., et al. (2009). PEI–PEG-chitosan-copolymer-coated iron oxide nanoparticles for safe gene delivery: Synthesis, complexation, and transfection. *Advanced Functional Materials*, *19*, 2244–2251.

Kircheis, R., Schuller, S., Brunner, S., Ogris, M., Heider, K. H., Zauner, W., et al. (1999). Poly-cation-based DNA complexes for tumor-targeted gene delivery in vivo. *The Journal of Gene Medicine*, *1*, 111–120.

Krezel, A., & Bal, W. (2003). Structure–function relationships in glutathione and its analogues. *Organic & Biomolecular Chemistry*, *1*, 3885–3890.

Kunath, K., Merdan, T., Hegener, O., Häberlein, H., & Kissel, T. (2003). Integrin targeting using RGD-PEI conjugates for in vitro gene transfer. *The Journal of Gene Medicine*, *5*, 588–599.

Landry, F. B., Bazile, D. V., Spenlehauer, G., Veillard, M., & Kreuter, J. (1996). Influence of coating agents on the degradation of poly(D,L-lactic acid) nanoparticles in model digestive fluids (USP XXII). *STP Pharma Sciences*, *6*, 195–202.

Leamon, C. P., & Low, P. S. (2001). Folate-mediated targeting: From diagnostics to drug and gene delivery. *Drug Discovery Today*, *6*, 44–51.

Lee, D., Zhang, W., Shirley, S. A., Kong, X., Hellermann, G. R., Lockey, R. F., et al. (2007). Thiolated chitosan/DNA nanocomplexes exhibit enhanced and sustained gene delivery. *Pharmaceutical Research*, *24*, 157–167.

Li, C. X., Guo, T. Y., Zhou, D. Z., Hu, Y. L., Zhou, H., Wang, S. F., et al. (2011). A novel glutathione modified chitosan conjugate for efficient gene delivery. *Journal of Controlled Release*, *154*, 177–188.

Loretz, B., Thaler, M., & Schnurch, A. B. (2007). Role of sulfhydryl groups in transfection? A case study with chitosan-nac nanoparticles. *Bioconjugate Chemistry*, *18*, 1028–1035.

Martien, R., Loretz, B., Thaler, M., Majzoob, S., & Schnürch, A. B. (2007). Chitosan-thioglycolic acid conjugate: An alternative carrier for oral nonviral gene delivery? *Journal of Biomedical Materials Research*, *82*, 1–9.

Mintzer, M. A., & Simanek, E. E. (2009). Nonviral vectors for gene delivery. *Chemical Reviews*, *109*, 259–302.

Morille, M., Passirani, C., Vonarbourg, A., Clavreul, A., & Benoit, J. P. (2008). Progress in developing cationic vectors for non-viral systemic gene therapy against cancer. *Biomaterials*, *29*, 3477–3496.

Muzzarelli, R. A. A. (2010). Chitosans: New vectors for gene therapy. In R. Ito, & Y. Matsuo (Eds.), *Hand book of carbohydrate polymers: Development, properties and applications* (pp. 583–604). Hauppauge, NY, USA: Nova Publisher.

Muzzarelli, R. A. A., Boudrant, J., Meyer, D., Manno, N., DeMarchis, M., & Paoletti, M. G. (2012). Current views on fungal chitin/chitosan, human chitinases, food preservation, glucans, pectins and inulin: A tribute to Henri Braconnot, precursor of the carbohydrate polymers science, on the chitin bicentennial. *Carbohydrate Polymers*, *87*, 995–1012.

Ogris, M., Brunner, S., Schuller, S., Kircheis, R., & Wagner, E. (1999). PEGylated DNA/trans-ferrin-PEI complexes: Reduced interaction with blood components, extended circulation in blood and potential for systemic gene delivery. *Gene Therapy*, *6*, 595–605.

Ogris, M., Walker, G., Blessing, T., Kircheis, R., Wolschek, M., & Wagner, E. (2003). Tumor-targeted gene therapy: Strategies for the preparation of ligand-polyethylene glycol-polyethylenimine/DNA complexes. *Journal of Controlled Release*, *91*, 173–181.

Oupicky, D., Ogris, M., & Seymour, L. W. (2002). Development of long-circulating poly-electrolyte complexes for systemic delivery of genes. *Journal of Drug Targeting*, *10*, 93–98.

Pack, D. W., Hoffman, A. S., Pun, S., & Stayton, P. S. (2005). Design and development of polymers for gene delivery. *Nature Reviews*, *4*, 581–593.

Ravi Kumar, M. N. V., Muzzarelli, R. A. A., Muzzarelli, C., Sashiwa, H., & Domb, A. J. (2004). Chitosan chemistry and pharmaceutical perspectives. *Chemical Reviews*, *104*, 6017–6084.

Rorke, S. O., Keeney, M., & Pandit, A. (2010). Non-viral polyplexes: Scaffold mediated delivery for gene therapy. *Progress in Polymer Science*, *35*, 441–458.

Salem, A. K., Searson, P. C., & Leong, K. W. (2003). Multifunctional nanorods for gene delivery. *Nature Materials*, *2*, 668–671.

Schmitz, T., Bravo-Osuna, I. B., Vauthier, C., Ponchel, G., Loretz, B., & Schnürch, A. B. (2007). Development and in vitro evaluation of a thiomer-based nanoparticulate gene delivery system. *Biomaterials*, *28*, 524–531.

Sun, C., Veiseh, O., Gunn, J., Chen, F., Hansen, S., Lee, D., et al. (2008). In vivo mri detection of gliomas by chlorotoxin-conjugated superparamagnetic nanoprobes. *Small*, *4*, 372–379.

Tian, H., Lin, L., Chen, X., Park, T. G., & Maruyama, A. (2011). RGD targeting hyaluronic acid coating system for PEI-PBLG polycation gene carriers. *Journal of Controlled Release*, *155*, 47–53.

Tian, Q., Zhang, C., Wang, X., Wang, W., Huang, W., Cha, R., et al. (2010). Glycyrrhetinic acid-modified chitosan/poly(ethylene glycol) nanoparticles for liver-targeted delivery. *Biomaterials*, *31*, 4748–4756.

Veiseh, O., Sun, C., Gunn, J., Kohler, N., Gabikian, P., Lee, D., et al. (2005). Optical and MRI multifunctional nanoprobe for targeting gliomas. *Nano Letters*, *5*, 1003–1008.

Zhang, C., Gao, S., Jiang, W., Lin, S., Du, F., Li, Z., et al. (2010). Targeted minicircle DNA delivery using folate-poly(ethyleneglycol)-polyethylenimine as non-viral carrier. *Biomaterials*, *31*, 6075–6608.

Zhao, X., Yin, L. C., Ding, J. Y., Tang, C., Gu, S. H., Yin, C. H., et al. (2010). Thiolated trimethyl chitosan nanocomplexes as gene carriers with high in vitro and in vivo transfection efficiency. *Journal of Controlled Release*, *144*, 46–54.